Some Properties of the Coercive Force in Soft Magnetic Materials

D. S. RODBELL AND C. P. BEAN
General Electric Research Laboratory, Schenectady, New York
(Received May 7, 1956)

The coercive force is the value of the magnetic field amplitude when the net magnetization in the direction of the field is zero and has a zero time rate of change. An equivalent definition of the coercive force is contained in the expression for the average instantaneous domain wall velocity; $v=k(H-H_c)$, in which k depends upon motional energy losses and H is the applied magnetic field: H_c is the coercive force. We have used this latter definition to measure the coercive force in specimens of magnetically annealed 65 Permalloy (65% Ni-Fe) tapes and a 3.25% SiFe picture frame single crystal for both low- and high-field domain configurations. The coercive force measured in this way for low applied fields is the same as that determined by other techniques. For the high-field determination, with domain walls unattached to the specimen surfaces, the coercive force is, for our samples, less than half the low-field coercive force. We call the value determined at high fields the "internal coercive force" and believe this value to be characteristic of the bulk material. The low-field coercive force includes both the "internal coercive force" and a component due to preferential "pinning" of domain walls at the specimen surfaces. The experimentally observed dependence of the coercive force upon specimen thickness may be explained using surface pinning of domain walls. This explanation was previously postulated by Dijkstra.

The difference in coercive force between surface free and surface pinned domain walls may be used to make a lower limit estimate of the domain wall energy density. The results are in order-of-magnitude agreement with the values expected from theory.

Considerations of the experimentally determined expression for domain wall velocity given above show that the positional free-energy variations which determine the coercive force cannot be described by conservative periodic functions.

INTRODUCTION

THE coercive force is a measure of the magnetic field necessary to reduce the net magnetization of ferromagnetic material from its saturation value in some selected direction to zero in that direction. In discussing the coercive force it is necessary to be specific regarding the way in which the magnetization changes since there are two mechanisms by which this may occur: by rotation of the net magnetization as a unit, or by the motion of domain walls. In a large class of materials—the so-called "soft magnetic materials"—changes of magnetization in a desired direction occur primarily by domain wall motion and since this is a low-energy process compared to rotation of the net magnetization, it is associated with small coercive fields (i.e., of about one oersted or less).

For purposes of clarity, what we shall mean by the coercive force in soft magnetic materials is the following. With respect to a selected reference direction for the net magnetization, we begin with the magnetization at its saturation value and define the coercive force as the magnetic field when the magnetization and the time rate of change of magnetization are each zero. All real measurements yield values which are approximations to this definition, but the difference can be made arbitrarily small in most cases.

The coercive force may be measured with good accuracy using a recording fluxmeter,[1] or by means of the more tedious point to point techniques. When the domain structure of the specimen is known, the coercive force may be determined by implication from domain wall velocity measurements. It has been shown experimentally[2–5] that the average instantaneous velocity of a domain wall under the influence of a magnetic field, H, may be described by

$$v=k(H-H_c), \tag{1}$$

where the mobility k depends upon the losses which limit the velocity of the moving domain wall, and H_c is the coercive force.

This article discusses two points that relate to the nature of the coercive force in soft magnetic materials. The first is an explanation of the observed dependence of the coercive force of magnetic sheet materials upon sheet thickness. The second point concerns the relationship (1) from which we conclude the type of position-dependent, free energy of a domain wall which determines the coercive force.

PART I. COERCIVE FORCE DEPENDENCE UPON SHEET THICKNESS

Evidence for the dependence of the coercive force upon the thickness of magnetic sheet materials has been presented by several investigators.[6–9] The observed behavior is that the coercive force increases approximately linearly with the reciprocal of the sheet thickness from the coercive force associated with an infinitely thick specimen. The materials studied have been sheets

[1] P. P. Cioffi, Phys. Rev. **67**, 200 (1945).

[2] K. H. Stewart, Colloquium on Ferromagnetism and Antiferromagnetism, Grenoble, France, 177, July, 1950.
[3] J. K. Galt, Bell System Tech. J. **133**, 1023 (1954).
[4] Williams, Shockley, and Kittel, Phys. Rev. **80**, 1090 (1950).
[5] C. P. Bean and D. S. Rodbell, J. Appl. Phys. **26**, 124 (1955).
[6] M. F. Littman, Trans. Am. Inst. Elec. Engrs. **71**, 220 (1952).
[7] U. P. Burdakova and V. V. Druzhinin, Zhur. Tekh. Fiz. **25**, 108 (1955).
[8] L. J. Dijkstra, *Thermodynamics in Physical Metallurgy* (American Society for Metals, Cleveland, 1953), p. 209.
[9] V. A. Zaikova and Y. S. Shur, Doklady Akad. Nauk (S.S.S.R.) **94**, 663 (1954).

of polycrystalline nickel-iron alloys, silicon-iron alloys of single and polycrystal structure, and nickel.

Burdakova and Druzhinin,[7] in an investigation of the increase in coercive force with decreasing thickness of silicon-iron specimens, suggested that the effect of rolling and subsequent treatment of the surface might be the cause of the increase in the measured coercive force. Their experimental results do not show that surface strain and oxidation are the major causes of the increased coercive force and their conclusion, like that of Zaikova and Shur,[9] considers the observed variation of the coercive force to be due to changes of the domain structure with thickness which allow different processes of remagnetization to occur. Feldtkeller[10] has measured initial permeabilities in magnetic sheet materials over a wide range of frequencies. Considerations of the "skin depth" enabled him to compare initial permeabilities in different regions of the specimen cross section. His results show that the initial permeability becomes extremely small at the surfaces compared to its value well within the specimen. Similar results have recently been reported by Gurvich and Kondorskii.[11]

It is the contention of the present article that the thickness-dependent coercive force arises from preferential pinning of domain walls at the sheet surfaces; a suggestion originally made by Dijkstra.[8]

Experimental Observations

Specimens of magnetically annealed 65 Permalloy (65% nickel-iron alloy) in tape form and "picture-frame" single crystals of silicon-iron have previously been shown to exhibit simple domain structures.[4,5,12,13] For small values of the applied magnetic field a single plane domain wall, parallel to the thin edge of the specimen, moves through the width of the specimen accomplishing the reversal of the magnetization. In some cases, it is possible to have two such narrow domain walls moving inward from opposite edges accomplishing the low field reversal. For much larger fields the reversal domain grows inward from all surfaces by means of a cylindrical domain wall. The important difference between these two behaviors (low- and high-field) relative to the present discussion is that in the high-field case the domain wall, once formed, is not in contact with the surfaces of the specimen. By employing Eq. (1), we may deduce the coercive force for (a) domain walls that contact the specimen surface, and (b) domain walls that do not contact the specimen surface.

The experimental procedure consists of placing a set of windings on the specimen and through one of these passing a current whose magnetic field is sufficient to magnetize the specimen to saturation. This field is removed, and at the same time another field in the opposite direction is applied through a second winding. The resulting change in magnetization as a function of time is observed on an oscilloscope via a third winding. The amplitude of the oscilloscope signal is proportional to the time rate of change of magnetization, and since the domain geometry is known, it is also proportional to the domain wall velocity. Measurement of the domain wall velocity in this way as a function of the applied magnetic field yields the necessary information to determine the coercive force from Eq. (1).

It is also possible to determine the coercive force by measurement of the time, T, required for the domain wall to move between fixed end points as a function of the applied magnetic field. Because it can be shown from Eq. (1) that the product $T(H-H_c)$ is a constant provided the domain wall retains its initial shape even when the mobility k depends upon domain wall position, it is possible to determine the coercive force from data of T^{-1} *versus* H.

Low-Field Behavior

It has been pointed out previously[5] that in the low-field range these tape specimens have in some regions two edge domain walls active and because of this the maximum amplitude of dB/dt will be twice that predicted for a single active wall. On the other hand, the total time for reversal is determined by the regions in which only one edge wall is active and should consequently agree with the predicted value based on a single edge wall picture. The prediction assumes eddy-current damping only and would be modified somewhat if account of other losses were made. Figures 1 and 2 show the observed and predicted behavior. The agree-

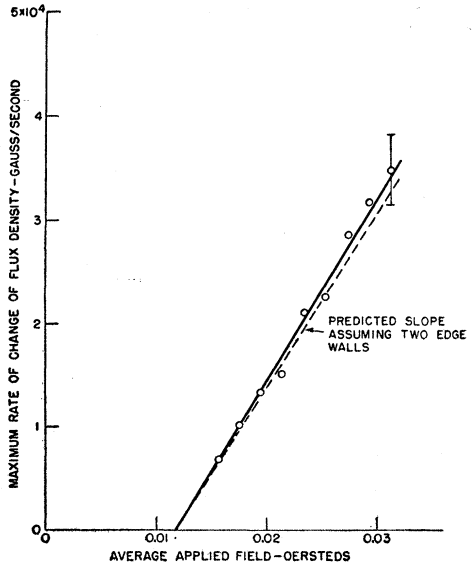

FIG. 1. Data from low-field reversal wave shapes of the 0.0047-inch 65 Permalloy tape specimen.

[10] R. Feldtkeller, Fernmelde Techn. Z. **2**, S 9/14 (1949).
[11] E. I. Gurvich and E. Kondorskii, Doklady Akad. Nauk (S.S.S.R.) **104**, No. 4, 530 (1955).
[12] H. J. Williams and W. Shockley, Phys. Rev. **75**, 178 (1949).
[13] D. S. Rodbell and C. P. Bean, J. Appl. Phys. **26**, 1318 (1955).

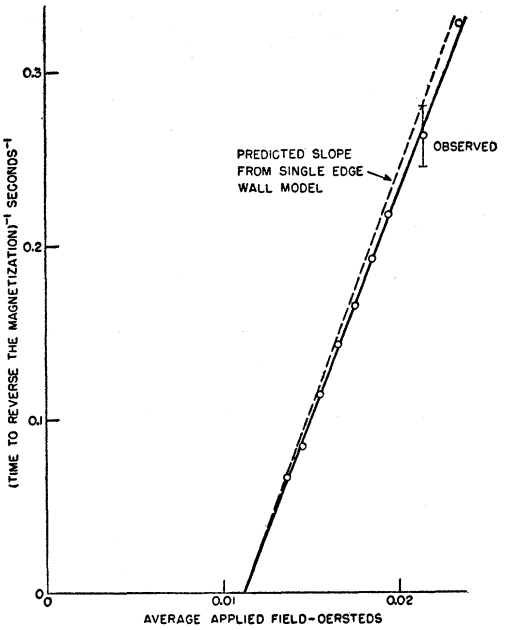

FIG. 2. Data from low-field reversal wave shapes of the 0.0047-inch 65 Permalloy tape specimen.

ment with prediction confirms the presumption that in the magnetic field range where the domain walls are essentially plane, the domain wall distribution remains the same and furthermore the coercive force may be determined by either observation of domain wall velocity or reversal time. The values obtained by these methods are in agreement with the results of dc hysteresograph determinations.

The determination of the coercive force of the silicon-iron picture-frame specimen by low-field measurements of dB/dt amplitudes is discussed in detail in Appendix 1. A value of $H_c=0.056$ oersted was obtained. The analysis in the appendix predicts a total time for the reversal of magnetization which is plotted as a function of magnetomotive force in Fig. 3, along with the experimental observations.

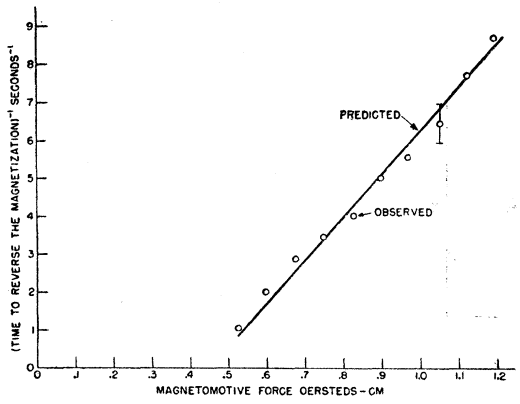

FIG. 3. The low-field behavior of the 3.25% silicon-iron picture frame specimen. The predicted curve uses $H_c=0.056$ oersted.

High-Field Behavior

The high-field domain configuration is a cylindrical domain wall that forms just inside the specimen surface and moves inward. The coercive force determination for this domain configuration is, in principle, identical with that for the low-field configuration. For example, once the cylindrical domain has been established, as by a high-field pulse, we may measure the time required for it to move a known distance in a known field, or its initial velocity following the formative pulse. The coercive force is determined, just as in the low-field case, by extrapolation of the data. We shall call the value obtained for the high-field domain configuration the "internal coercive force," H_c^{int}.

The desired cylindrical domain is formed by a short-duration, high-amplitude magnetic field pulse. This pulse must have a longer duration than the "nucleation time" of the cylindrical domain, but a shorter duration than the time for total reversal corresponding to the amplitude of the pulse field.[13] Once formed, the cylindrical domain wall may be driven inward or outward by small-amplitude magnetic fields. In either case, we assume that the initial velocity is

$$v=k'(H-H_c^{\text{int}}), \tag{2}$$

a form similar to Eq. (1). The constant of proportionality in this case, however, depends upon the starting position[13] since the further in the domain has grown the larger the eddy currents, which are the major limitation of the wall's velocity. The starting position is determined by the formative pulse duration and amplitude. By employing pulses of different duration, at the same amplitude, the starting position may be changed and consequently k' will change.

The initial velocity data of Figs. 4 and 5 are obtained from measurements with the silicon-iron specimen and the 0.0047-inch Permalloy tape respectively. The several pulse durations used yield, within experimental error, the same value of H_c^{int}. In addition, the intercepts and slopes obtained for both positive and negative background fields are equal for the same formative pulse, indicating that there is no directional character in the mobility of the domain walls.[14]

[14] The effective field associated with change in length of a domain wall as it moves results from the change in the stored energy of the domain wall. This effective field has the value $\gamma/2I_s r$, where γ is the domain wall energy per unit area, I_s is the saturation magnetization, and r is the radius of curvature. For increasing r, the effective field opposes the motion while for decreasing r, the effective field assists the motion. For the specimens considered here in the high-field domain configuration, the effective field acting on the broad wall sections is of the order of 10^{-4} oersted for the Permalloy tapes and 10^{-3} oersted for the silicon-iron specimen. Both magnitudes are within the limits of experimental error and consequently directional effects due to them are not observed by the techniques employed. Domain wall "spikes" between the specimen surfaces and the cylindrical domain wall could conceivably contribute to a directional character of the mobility, i.e., resisting inward motion, but assisting outward domain wall motion. Our data do not indicate such effects.

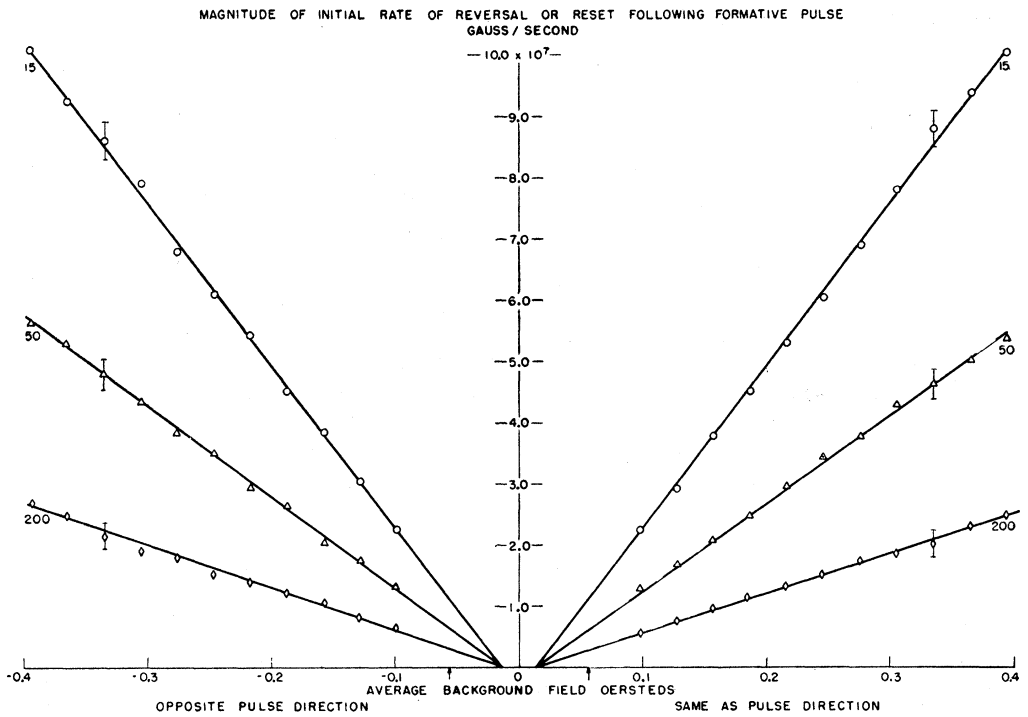

FIG. 4. The initial velocity behavior of the high-field cylindrical domain configuration as a function of small amplitude background fields for the 3.25% silicon-iron picture frame specimen. The numbers associated with each curve are the pulse duration in microseconds. The formative peak time for this pulse amplitude is 1 μsec and the pulse amplitude, if sustained, would reverse the magnetization in 360 μsec.

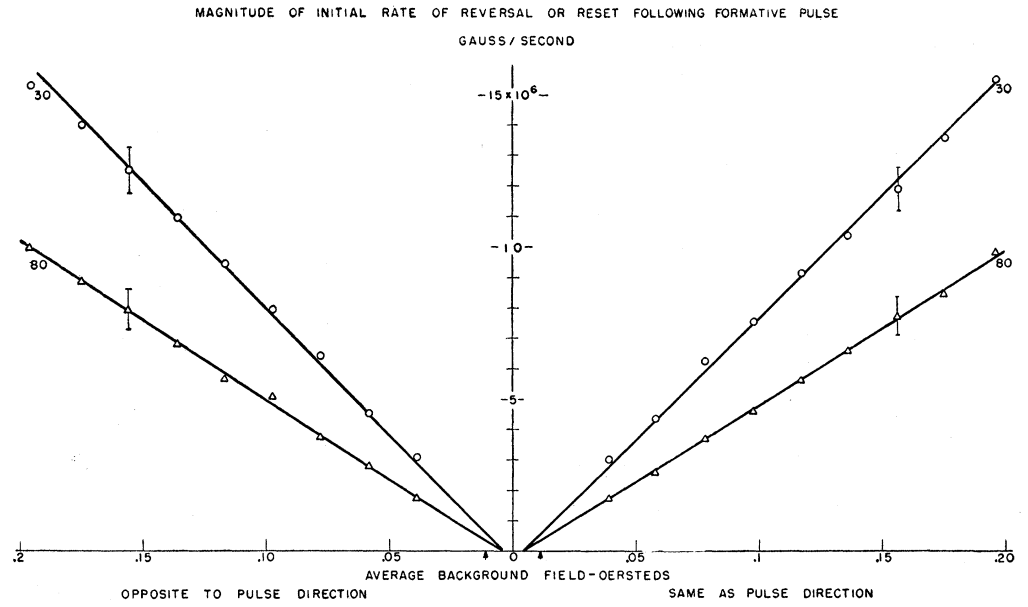

FIG. 5. The initial velocity behavior of the high-field cylindrical domain configuration as a function of small amplitude background fields for the 0.0047-inch 65 Permalloy tape specimen. The numbers associated with each curve are the pulse duration in microseconds. The formative peak time for this pulse amplitude is 5 microseconds and this pulse amplitude, if sustained, would reverse the magnetization in 160 μsec. The arrows on the abscissa indicate the low-field-determined coercive force.

As mentioned earlier, the time for the cylindrical domain wall to travel inward to completion of the reversal, or outward to the surface, may also be used to determine the internal coercive force. The reciprocal of these times should be proportional to $(H-H_c^{\text{int}})$. The constant of proportionality depends not only upon the starting position of the domain wall, but also upon its final position. This means that the data for inward motion need not have the same slope as that for outward motion.

In addition, we must restrict the time measurements to fields whose amplitudes are small enough so that no new domain structures are formed. It is possible, for example, with large fields that tend to move the cylindrical domain wall out to the surface, to grow a new inward-moving domain at the surface. This additional domain wall masks the desired reset time so that it cannot be determined. Results of time measurements are shown in Fig. 6 for the 0.0047-inch 65 Permalloy specimen. In the observation of the reset (outward motion) time there is a characteristic "denucleation" peak in the dB/dt wave shape; we believe this to be the result of the domain wall's annihilation at the specimen surface. It is the time between the termination of the formative pulse and this "denucleation" peak which is measured as the reset time. Justification for the use of the "denucleation" peak is given in Fig. 7 which compares initial-amplitude data with "denucleation" peak time observations for the 0.0047-inch 65 Permalloy specimen. The agreement between the determination of H_c^{int} by the two methods substantiates the assumption that the "denucleation" peak corresponds to a fixed position near the surface of the specimen and that this position is independent of the initial position of the cylindrical domain wall.

We return to Fig. 6 to point out an interesting fact. The value of H_c^{int} obtained by extrapolating the curve for continued inward motion of the domain wall (the dashed line) gives the same result as the extrapolated reset-time data. The interesting fact is that the data for very small background fields departs markedly from the continued inward extrapolation and one observes "continued inward" behavior even for small negative background fields. We believe this behavior is due to the narrow end-wall sections of the cylindrical domain wall. These end-wall sections have their minimum radius of curvature determined by the separation of the broad wall sections. The curvature of the end walls has associated with it an effective magnetic field which is inversely proportional to the radius of curvature and which tends to drive the end walls inward. The net field acting on the end walls exceeds the applied field by this effective field. The result is that for sufficiently small applied fields, the broad domain wall sections move slowly inward while the end-wall sections move very rapidly through the specimen because of their enhanced driving field and it is, therefore, the motion of the end walls that determines the reversal time. The intercept of the data in the region where the end walls appear to control the reversal time, should be equal to $(H_\gamma-H_c^{\text{int}})$ where H_γ is the effective field at the end walls. We shall return to this point in a later section.

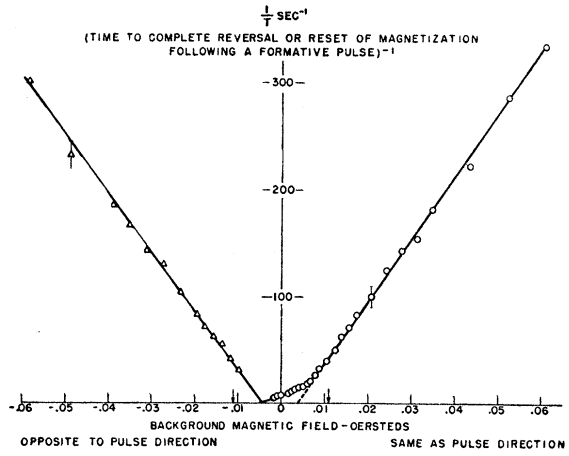

FIG. 6. The time behavior of the high-field cylindrical domain configuration as a function of small-amplitude background fields for the 0.0047-inch 65 Permalloy tape specimen. A formative pulse duration of 100 microseconds establishes the high-field domain configuration. The formative peak time for this pulse amplitude is 6 μsec and if sustained, this pulse amplitude would reverse the magnetization in 180 μsec. The arrows on the abscissa indicate the low-field-determined coercive force.

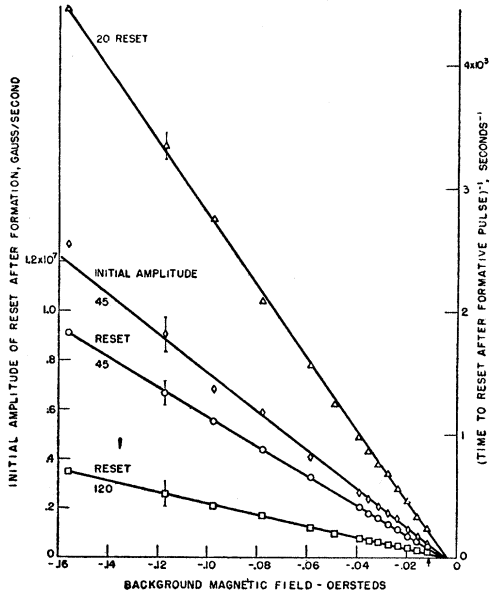

FIG. 7. Comparison of initial-amplitude and reset-time behavior of the high-field cylindrical domain configuration for the 0.0047-inch 65 Permalloy tape specimen. The formative pulse durations employed are noted in microseconds on each curve. The pulse amplitude results in a formative peak time of 6 microseconds and, if sustained, this pulse amplitude would reverse the magnetization in 180 μsec. The low-field-determined coercive force is noted by the arrow on the abscissa.

TABLE I. *Summary of pertinent data.* Unless otherwise noted, the values apply to room temperature (20°C).

Specimen	Composition	Form	Resistivity micro-ohm-cm	B_s gauss $\times 10^4$	H_c oersteds (surface attached domain walls)	H_c^{int} oersteds (domain walls unattached to specimen surface)	Estimate of domain wall energy density ergs/cm² [using Eq. (5)]
Permalloy tapes (0.5 in. wide) 0.0098 in. thick (0.0249 cm)	64% Ni, 1% Mo, Fe	13-wrap toroid 4.1 cm av diam	41.7	1.27	$0.014_5 \pm 0.001$	$0.005_9 \pm 0.002$	0.21 ± 0.08
0.0047 in. thick (0.0119 cm)	65% Ni-Fe	29-wrap toroid 4.1 cm av diam	20.7	1.29	0.011 ± 0.001 (0.018 ± 0.001)[b]	$0.004_4 \pm 0.001$ (0.0069 ± 0.001)[b]	0.08 ± 0.025 ($0.13_5 \pm 0.025$)[b]
0.0028 in. thick (0.0071 cm)	65% Ni-Fe	45-wrap toroid 4.1_2 cm av diam	21.7	1.31	$0.011_5 \pm 0.001$	$0.003_1 \pm 0.001$	$0.06_3 \pm 0.025$
Silicon-iron[a]	3.25% Si-Fe	Pict. frame[a]	47.0	1.7_5	0.056 ± 0.006	0.015 ± 0.005	3.0 ± 0.8

[a] See Fig. 1, Appendix 1.
[b] Determined at liquid nitrogen temperature (−196°C).

A summary of the values of the low-field coercive force H_c corresponding to domain walls that contact the specimen surface and the coercive force for cylindrical domain walls, H_c^{int}, is given in Table I for the specimens measured.

Discussion

Before discussing the experimental results, let us briefly review the present theories of coercive force. A system composed of a magnetic specimen containing a domain wall has a free energy that depends upon the location of the domain wall within the specimen. From a fundamental point of view, the coercive force measures the maximum rate of change of this free energy with position. Reviews of current theories on the origin of the coercive force have been given by Kittel,[15] Dijkstra,[8] and Kersten.[16] It is believed that the major contributions to this energy variation arise from the effects of inclusions, cavities, and stresses. For example, stresses may be considered to change the local value of the anisotropy constant via magnetostriction and consequently the surface energy density of the domain wall is changed locally. Nonmagnetic inclusions and cavities contribute to mechanical stresses, but in addition contribute to the energy of the system in a manner which depends upon the size of the inhomogeneity with respect to the domain wall thickness. Very small inhomogeneities inhibit the passage of a domain wall, because the energy stored within a domain wall surrounding such a region is smaller than an undisturbed domain wall and consequently the system energy must be increased to enable the domain wall to pass. Similar contributions are made by inhomogeneities whose size is larger than the domain wall thickness, the coercive force for particles which are less than the domain wall thickness increases with particle size, whereas the coercive force due to large particles decreases with increasing particle size.

[15] C. Kittel, Revs. Modern Phys. **21**, 541 (1949).
[16] M. Kersten, Z. angew. Phys. **7**, 397 (1955).

Magnetic inhomogeneities which are large in comparison with the domain wall thickness have in addition to the effects mentioned above, a large magnetostatic energy due to the magnetic pole density at their surfaces, which is reduced when a domain wall is located at their position as has been pointed out by Néel.[17] Considerations of the energy involved in such large cavities leads to the prediction of closure domain spikes which allow the specimen magnetization to jog past the inhomogeneity with only small magnetostatic energy resulting at the interface. The existence of these spikes in silicon-iron specimens has been established[12] by using colloid techniques, which also show that as a domain wall passes such sites the closure spikes are dragged along for a considerable distance before they snap free and resume their equilibrium configuration. The stretching of these domain spikes requires energy which is not returned to assist the domain wall motion, but is dissipated when the spike snaps free and, therefore, contributes to a free-energy variation of the specimen with domain wall position which is nonconservative. Part II of this paper elaborates upon this point.

The contributions from the above mechanisms are believed to be the major sources of the "coercive force" in bulk materials, and without them the coercive force would be extremely small for the usual domain wall structures.

We now consider the contribution to the net coercive force from surface pinning. A magnetic material in sheet form of thickness a, containing two antiparallel domains which are separated by a domain wall that is normal to the broad sheet surfaces, will have, as the result of the effects mentioned above, a coercive force which is characteristic of the bulk material, H_c^{int}. Let us suppose that at some positions along the surfaces of the sheet the domain wall may be pinned, and in order to move the wall we must apply a magnetic field

[17] L. Néel, Cahiers phys. **25**, 21 (1944).

in excess of H_c^{int}. The maximum extra contribution to the coercive force due to surface pinning is

$$H_c^{\text{surf}}=\gamma/I_s a, \tag{3}$$

since at this field the domain wall is bowed sufficiently to be tangent to the surface and thus escape the pinning points. The total coercive force then becomes

$$H_c=H_c^{\text{int}}+\beta H_c^{\text{surf}}. \tag{4}$$

The parameter β has the range $0\leq\beta\leq 1$, its value depending upon the extent of the surface pinning; i.e., if the domain wall is pinned entirely along both sheet surfaces, then $\beta=1$ and complete lack of pinning gives $\beta=0$. Since there is no clear procedure to determine what value to assign to β, nothing more definite may be said about it. We note in passing that Eqs. (3) and (4) are in formal agreement with expressions given by Dijkstra[8] in his discussion of the dependence of coercive force on specimen thickness.

It is possible from our data to make an estimate of the lower limit of the domain wall energy density, γ. By setting $\beta=1$, we obtain this estimate in the following way. From (3) and (4) we have

$$\gamma=(H_c-H_c^{\text{int}})I_s a. \tag{5}$$

Using the tabulated values of the quantities indicated, we may evaluate γ, and since we have chosen $\beta=1$, this is a lower limit estimate. The result for the 65 Permalloy specimens is about 0.1 erg/cm^2 and for the silicon-iron specimen 3.0 ± 0.8 ergs/cm^2 (see Table I). The latter value may be 15% too high since the difference in surface energy density between {100} and {110} domain walls has been neglected in this estimate.

The treatment we have described should not be expected to yield better than order of magnitude estimates. We interpret the agreement in order of magnitude obtained from our data with that expected from theory to be confirmative evidence for the plausibility of the surface-pinning contribution to the coercive force.

In the above treatment we have not specified what the pinning sites are except that their location is at the specimen surfaces. There may be pinning sites throughout the volume also, but their contribution is contained in the parameter H_c^{int}. A possible mechanism for the surface pinning could be the following: When the magnetization within a domain wall intersects the sheet surface, the magnetostatic energy is greater for surface regions which are normal to the domain wall than for those which are not. Consequently, the wall prefers irregular surface regions and may be pinned at such locations.

Néel[18] has recently considered this magnetostatic energy in the case of plane sheet surfaces normal to domain walls. His result shows that there can be an apparent variation in domain wall energy density with sheet thickness caused by this magnetostatic energy. In particular, the apparent domain wall energy density γ' increases as the specimen thickness decreases, attaining a maximum when the specimen thickness equals the domain wall thickness δ; and below this value of specimen thickness, γ' decreases with decreasing thickness. We do not believe that this apparent wall energy is observed by techniques which deduce the wall energy from effects of domain wall curvature. The reason is that the magnetostatic energy responsible for γ' is localized to about a depth δ from the termination of the domain wall. Since domain wall curvature experiments involve domain walls whose linear dimensions are much greater than the domain wall thickness, the rate of change of the total wall energy with respect to its curvature due to any magnetostatic contribution at the wall ends becomes quite small.

The magnetostatic energy at the intersection of a domain wall and a surface, however, may be quite effective as a pinning site, because small variations in the angle that a domain wall makes with the surface make large changes in the magnetostatic energy. It is the rate of change of this energy with the wall's position which determines the effectiveness of the pinning, if one assumes that the over-all dimensions of the domain wall are constant.

In an earlier section we have mentioned a method of determining the effective field resulting from the domain-wall surface energy density. This determination involves the data of Fig. 6, in which we have noted that the time to complete the reversal of magnetization following a formative pulse is determined for very small background fields by the narrow edge walls of the cylindrical domain configuration. The applied magnetic field opposing the continued inward motion is aided by the internal coercive force, and this combined effect is overcome by the effective field at the edge walls owing to their surface energy and curvature. The applied field corresponding to the intercept at the abscissa is just equal to $H_\gamma-H_c^{\text{int}}$. The internal coercive force, H_c^{int}, has already been obtained and we therefore determine the value of H_γ, which is set equal to $\gamma/I_s d$. The dimension d in this case is the separation between the two broad domain walls of the cylindrical configuration and may be obtained by measurement of the remagnetization accomplished by the formative field pulse in comparison with the remagnetization corresponding to a complete reversal of the magnetization; i.e., $2B_s$. The resulting values from data for the 0.0047-inch 65 Permalloy specimen and data obtained for the silicon-iron specimen yield the result that γ (Permalloy) is 0.03 ± 0.01 ergs/cm^2, while γ (silicon-iron) is 1.5 ± 0.5 ergs/cm^2. The significance of these results is again only in order of magnitude since we cannot account in

[18] L. Néel, Compt. rend. **241**, 533 (1955).

detail for the observed behavior in this low-field, continued inward, region.

We close this section with a remark concerning the dependence of coercive force upon temperature. Measurements made at the temperature of liquid nitrogen (−196°C) with the 0.0047-inch 65 Permalloy specimen indicate the coercive force to be higher than determinations by the same techniques at room temperature (see Table I). Moreover, the difference between the coercive force, H_c, and the internal coercive force, H_c^{int}, is greater than that at room temperature. If the point of view of surface pinning is correct in accounting for the difference between H_c and H_c^{int}, and we assume that the pinning sites are temperature independent, then we may interpret these results to be due to an increase in the surface energy density of the domain wall at this lower temperature. This interpretation predicts a magnetocrystalline anisotropy constant at −196°C, which is a factor of three greater than the room temperature value. The exchange stiffness is assumed constant for temperatures well below the Curie point.

PART II. ORIGIN OF THE COERCIVE FORCE

It does not appear to have been pointed out previously that the experimentally determined relationship [Eq. (1)] between the average domain wall velocity and applied magnetic field, casts some light upon the origin of the coercive force.

The concept of an internal field derivable from a periodic free energy distribution may be generalized in the following way. The internal field, to within a constant factor C, is

$$H_{\text{internal}}=-C(\partial W/\partial x), \tag{6}$$

where $\partial W/\partial x$ is the positional variation of the internal energy.

If d_0 is the repetition distance characteristic of the free-energy variations, and the instantaneous motion of the domain wall is assumed to be controlled by damping, i.e.,

$$v=\alpha(H+H_{\text{internal}}), \tag{7}$$

then the average velocity as a function of the applied external field, H, is

$$\bar{v}=\alpha d_0\Big/\int_0^{d_0}\frac{dx}{H+H_{\text{int}}}. \tag{8}$$

For applied fields, H, which are large compared to H_{internal}, the approximation given below may be made (to second order);

$$\bar{v}\doteq\alpha d_0 H\Big/\int_0^{d_0}\left[1-\frac{H_{\text{int}}}{H}+\left(\frac{H_{\text{int}}}{H}\right)^2\right]dx. \tag{9}$$

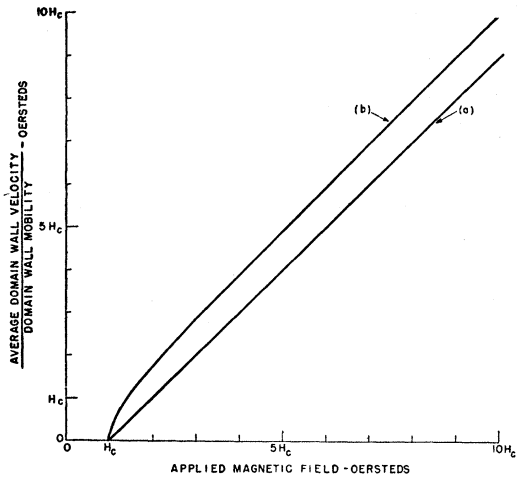

FIG. 8. Dependence of the average domain wall velocity upon applied magnetic field: (a) experimentally observed; (b) predicted using a sinusoidal internal field. The ordinate is plotted in reduced units.

Because W is periodic, the second term in the brackets vanishes when integrated, with the resulting expression

$$\bar{v}\doteq\alpha H\left[1-\frac{1}{d_0}\int_0^{d_0}\left(\frac{H_{\text{int}}}{H}\right)^2\right]dx, \tag{10}$$

which is of the form

$$\bar{v}\doteq\alpha[H-O(H_c^2/H)]. \tag{11}$$

A special case is now treated by the assumption (which is often made) of a sinusoidal dependence of the free energy of a ferromagnet with domain wall position. In this case, the form of the effective internal field is

$$H_{\text{internal}}=-H_c\sin(2\pi x/d_0). \tag{12}$$

The average velocity predicted, without approximation, is, from (8),

$$\bar{v}=\alpha(H^2-H_c^2)^{\frac{1}{2}}, \tag{13}$$

the last expression being quite distinguishable from the experimentally observed results described in Eq. (1). For comparative purposes, Eqs. (1) and (13) are plotted in Fig. 8 as curves (a) and (b), respectively. In Eq. (13) the retarding force, in the approximation of high fields, is of the form H_c^2/H, as is to be expected from Eq. (11). The results of a periodic-type conservative energy distribution are clearly in disagreement with experiment.

A consequence of the assumption of a conservative field, as pointed out by Stewart,[2] is that conceptually a material may be magnetized with no net energy loss by the external magnetic field. One need only adjust the magnitude of the applied field to keep the instantaneous rate of magnetization zero. In a discussion following the paper of reference 2, Shockley pointed out that Néel spikes, attached to a domain wall and

dragged out by it, will not allow of this description and provide an intrinsically dissipative system. It seems reasonable to believe that any distortion of the domain wall and consequent snapping following its release from pinning centers will result in similar dissipation. The net effect is that after the domain wall has moved a sufficient distance to be in steady state, it will be under the influence of a constant frictional force, H_c, and this is adequate to explain the observed dependence of the average domain wall velocity upon magnetic field.

CONCLUSIONS

The coercive force as normally determined may be composed of the sum of two terms. The first is characteristic of the bulk material or for domain walls free of surface effects; the second is dimensionally dependent and arises from pinning of domain walls at the specimen surfaces. The results obtained may be used to explain the observed increase in coercive force with decrease in sheet specimen thickness and in addition account for the effects of background fields, smaller than the normal coercive force, on the pulsed reversals of magnetization previously described.[13]

Lastly, the velocity of the domain wall as a function of field indicates the motion of the domain wall to be a basically dissipative process, in particular this motion cannot be derived from a periodic conservative energy function.

ACKNOWLEDGMENTS

It is a pleasure to acknowledge the many valuable discussions related to this paper that we have had with our colleagues; in particular, we wish to thank E. W. Hart for his helpful comments and suggestions.

APPENDIX I

We consider below the "picture frame" geometry of the silicon-iron single crystal and the determination of the coercive force from low-field observations with this specimen. Figure 9 represents this crystal which is cut so that all surfaces are {100} planes. The magnetic behavior of such a crystal, when properly treated, is to support a simple domain geometry.[12] The sketch shows the crystal in a nonsaturated magnetic condition indicated by the 180° domain walls which follow the path p. At each corner, there is a 90° domain wall which eliminates demagnetization effects at the ends of the eight domains since these 90° domain walls allow the magnetization to change direction in a continuous manner.

When a magnetomotive force is applied by passage of a current i through N turns surrounding the specimen legs, the magnetic field along a path p is determined from

$$\oint_p \mathbf{H}\cdot d\mathbf{l}=4\pi Ni \text{ in Gaussian units.} \qquad (1)$$

Because of the manner in which the crystal is oriented, the magnetization will find the minimum energy directions to be parallel to the specimen surfaces and the magnetic field contours are coincident with these directions from the additional requirement that $\mathrm{div}\bar{B}=0$. The magnetic field at a position x (indicated in Fig. 9) will produce a velocity of the domain wall given by

$$v(x)=K_1[H(x)-H_c], \qquad (2)$$

where $K_1=\pi^2c^2\rho/33.6B_sa$, for the case of eddy current damping[4,13] only, and the magnetic field has the value

$$H(x)=\frac{4\pi Ni}{8(x+x_0)}=\frac{K_2}{(x+x_0)}. \qquad (3)$$

We now consider a domain wall originating at the inner edge of the picture frame and determine the time T_1 for it to travel the width L of the specimen leg. We neglect in this consideration the effective field

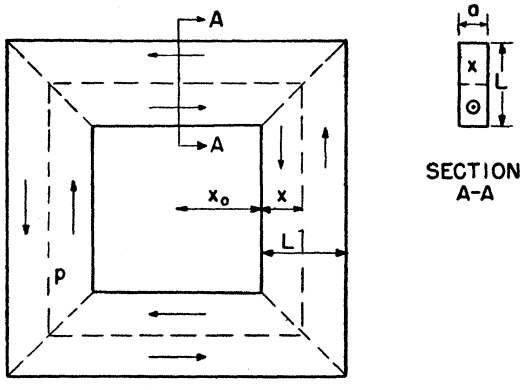

FIG. 9. The 3.25% silicon-iron specimen. The surfaces are oriented to be {100}. The outside length of each leg is 2.26_0 cm with $L=0.36_4$ cm and $a=0.051_8$ cm. The dashed lines represent domain walls.

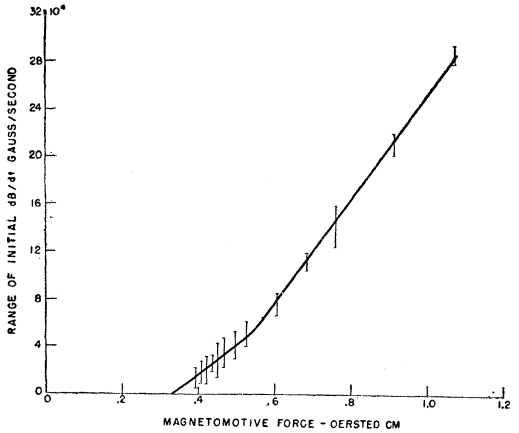

FIG. 10. The low-field behavior of the 3.25% silicon-iron picture frame specimen.

resulting from the increase in the domain wall length as the motion progress; the approximate value of this field is 10^{-4} oersted. We further assume that each of the four specimen legs will behave identically.

On combining (2) and (3) above, the result

$$dt=\frac{x+x_0}{K-C(x+x_0)}dx \tag{4}$$

is obtained. Integration of (4) yields the time

$$T_1=\frac{K_2}{K_1H_c^2}\ln\left\{\frac{(K_2-x_0H_c)}{K_2-(L+x_0)H_c}\right\}-\frac{L}{K_1H_c} \tag{5}$$

required for a domain wall to travel the width L of the specimen leg.

It appears evident from observations of the initial amplitude of the reversal wave shapes, that in addition to the inner wall moving outward there is also an outer edge wall moving inward. Figure 10 presents this evidence as a plot of the initial amplitude of dB/dt as a function of the applied magnetomotive force. The contributions to this amplitude are from the initial velocities of the domain walls as they begin their respective motions. We interpret the change of slope to correspond to the value of magnetomotive force for which the magnetic field at the outside edge of the specimen is not sufficient to grow and move a domain wall. For values of magnetomotive force less than this, only the inner edge wall is operative. The slope of the data in this region becomes about one-half that in the higher range of magnetomotive force, giving qualitative confirmation of this interpretation.

We may estimate the coercive force from this data in the following way: The field at the outer edge of the specimen corresponding to the change in slope of the data is 0.05_3 oersted. The field at the inner edge of the specimen corresponding to the zero dB/dt intercept is 0.05_9 oersted and is associated with the value of field for which a domain wall will not move from the inner edge of the specimen. Since the spread in the data is sufficient to account for the difference, we shall use the value 0.05_6 oersted as the edge-wall-determined coercive force. This value agrees with determinations made on a dc recording fluxmeter and, as we shall see below, predictions based on Eq. (5) employing this H_c are closely followed by experimentally determined reversal times.

From the foregoing discussion, it appears that we must correct Eq. (5) to account for both edge walls and, in addition, experimental comparison with predictions from this corrected equation may be made only above the minimum mmf which allows both walls to be operative. For smaller values of the applied mmf the inner edge wall may move, but it cannot completely reverse the magnetization since at some position the magnetic field will fall below the value of the coercive force.

For the situation of two noninteracting domain walls moving towards each other, having started at the same time from opposite edges of the specimen leg, the times elapsed for each motion when the walls meet must be identical. This time is the reversal time. We will label it T_2 and call the position at which the walls meet x_m. Returning to Eq. (4) with the substitution $\chi=x+x_0$, we may write the following for the inner wall:

$$\int_0^{T_2}dt=\int_{x_0}^{x_0+x_m}\frac{\chi}{K-C\chi}d\chi \tag{6}$$

and for the outer wall

$$\int_0^{T_2}dt=\int_{x_0+L}^{x_0+x_m}\frac{\chi}{K-C\chi}(-d\chi)=\int_{x_0+x_m}^{x_0+L}\frac{\chi}{K-C\chi}d\chi. \tag{7}$$

On addition of (6) and (7), we obtain

$$2\int_0^{T_2}dt=\int_{x_0}^{x_0+L}\frac{\chi}{K-C\chi}d\chi. \tag{8}$$

Identifying the right-hand side of (8) as T_1 from (4), the result is that

$$T_2=\tfrac{1}{2}T_1,$$

i.e., the time for reversal by two walls is precisely one-half that required by one wall.

This result may be used to predict the time of reversal as a function of the applied magnetomotive force from (5). Upon using $H_c=0.05_6$ oersted and evaluating K_1 to be 15.2_5 cm/sec oersteds ($B_s=17.5\times10^3$ gauss; $\rho=47\times10^{-6}$ ohm cm), the values of the predicted reversal time for two walls are plotted in Fig. 3 of this paper along with the experimentally observed values. The agreement of the data with prediction is taken as confirmation of the assumptions made and of the value of the coercive force used.